
Target-Aligned Reinforcement Learning

Leonard S. Pleiss¹ James Harrison² Maximilian Schiffer¹

Abstract

Many reinforcement learning algorithms rely on target networks—lagged copies of the online network—to stabilize training. While effective, this mechanism introduces a fundamental stability-recency tradeoff: slower target updates improve stability but reduce the recency of learning signals, hindering convergence speed. We propose Target-Aligned Reinforcement Learning (TARL), a framework that emphasizes transitions for which the target and online network estimates are highly aligned. By focusing updates on well-aligned targets, TARL mitigates the adverse effects of stale target estimates while retaining the stabilizing benefits of target networks. We provide a theoretical analysis demonstrating that target alignment correction accelerates convergence, and empirically demonstrate consistent improvements over standard reinforcement learning algorithms across various benchmark environments.

1. Introduction

In Reinforcement Learning (RL), agents optimize their policy through repeated interaction with an environment, aiming to maximize expected cumulative return. A central mechanism enabling this process is Temporal Difference (TD) learning (Sutton, 1988), which relies on bootstrapped target estimates—so-called target values. Current state estimates are iteratively updated toward the estimates of future states, thereby allowing the agent to anticipate long-term reward.

However, as shown by Mnih et al. (2015), naïvely using the online network to produce target values can destabilize learning. To address this issue, they introduced a designated target network. A target network is a lagged copy of the online network used exclusively to generate target values. By decoupling the online parameter updates from target value computation, the bootstrapped targets are generated by a comparatively stationary function approximator. This

reduces temporal correlations between updates and targets, suppresses self-reinforcing error feedback, and substantially improves training stability and convergence behavior. This innovation contributed to landmark achievements such as human-level performance on the Atari-57 benchmark (Mnih et al., 2015), and target networks remain a cornerstone of many state-of-the-art RL algorithms (Fujimoto et al., 2018; Badia et al., 2020; Hessel et al., 2017; Haarnoja et al., 2018; Badia et al., 2020; Schwarzer et al., 2023).

Despite their massive success, target networks introduce a critical limitation: by construction, their estimates are lagged relative to the online network. The lag can cause target estimates to become stale, reflecting outdated value predictions that no longer align with the current policy or representation (Vincent et al., 2025). In essence, it creates a dynamic analogous to aiming at a moving target using delayed coordinates: if the value function changes direction, the lagged target steers the update astray. Consequently, improved target stability necessarily comes at the cost of reduced recency, while increasing recency risks reintroducing instability. This phenomenon constitutes the fundamental *stability-recency tradeoff*: Ideally, target values should be as up-to-date as possible while preserving the level of stability required for reliable bootstrapped learning.

In this work, we argue that sacrificing recency is not necessary to ensure stability. We propose to circumvent this tradeoff by using the unstable but recent online network to validate the stable but partially stale target network. Our approach—Target-Aligned Reinforcement Learning (TARL)—prioritizes updates where online and target estimates agree, enabling the agent to exploit recent information without compromising stability.

Background Even though individual papers have recently claimed to bypass the need for a target network by proposing alternate update rules (Kim et al., 2019), functional regularization (Piché et al., 2023), decision transformers (Chen et al., 2021) or streaming algorithms (Elsayed et al., 2024), target networks remain widely used. They are a core component in most popular RL algorithms, including Deep Q-Network (DQN), Rainbow, Soft Actor-Critic (SAC) or Deep Deterministic Policy Gradient (Fujimoto et al., 2018; Hessel et al., 2017; Mnih et al., 2015; Haarnoja et al., 2018). Target networks further remain a cornerstone of state-of-the-

¹Technical University of Munich ²Google Research. Correspondence to: Leonard S. Pleiss <leonard.pleiss@tum.de>.

art RL algorithms to this day (Badia et al., 2020; Hessel et al., 2017; Haarnoja et al., 2018; Schwarzer et al., 2023).

As such, the stability-recency tradeoff is a fundamental consideration in RL, particularly during hyperparameter tuning. Most algorithms navigate the tradeoff through design choices that govern the target network’s update mechanism and cadence. There are two major update mechanisms, *hard* and *soft* target network updates (Li, 2023).

Methods like DQN (Mnih et al., 2015) or Rainbow (Hessel et al., 2017) traditionally perform *hard* updates. In some fixed frequency—denoted as the target update interval K —the target network is overwritten by the online network. This frequency is then tuned to balance stability and recency.

Other algorithms like SAC or Deep Deterministic Policy Gradient usually perform *soft* updates (Lillicrap et al., 2015; Kobayashi & Ilboudo, 2021; Haarnoja et al., 2018; Zhang et al., 2021). A soft update is a mechanism to incrementally adjust the target network’s parameters toward those of the online network. Rather than copying parameters at fixed intervals, the target network is gradually updated at every step. These gradual updates are usually performed via exponential moving or Polyak averages (Polyak & Juditsky, 1992), typically of the form

$$\theta_{\text{target}} \leftarrow \tau \theta_{\text{online}} + (1 - \tau) \theta_{\text{target}}, \quad (1)$$

where $\tau \in (0, 1]$ controls the update magnitude. Soft updates reduce the variance and non-stationarity of bootstrapped targets by smoothing parameter changes over time, improving training stability while still allowing target estimates to track the evolving online network.

Regardless of whether frequent soft updates or infrequent hard updates are employed, the challenge remains the same: to identify an optimal balance where stability is maintained while recency is maximized. Current methods therefore essentially treat this tradeoff as a zero-sum game, merely adjusting the slider between stability (low τ or high K) and recency (high τ or low K).

In contrast, we approach this challenge from a novel angle. We posit that we do not need to make the target network fresher (and more unstable) to improve learning; we only need to filter out updates where the target network’s staleness leads to incorrect update directions. We thus focus on the alignment between the stable estimate—the target network—and the most recent estimate—the online network—on a per-transition basis. We propose to prioritize updates where both target estimates are well-aligned, indicating that our learning target is both stable *and* recent. This perspective bypasses the conventional tradeoff, as it preserves stability without sacrificing recency.

Contribution Our contribution is fourfold: First, we introduce a novel offline-online target alignment metric that quantifies agreement between the online and target network value estimates. Second, we present TARK, an algorithmic framework that integrates target alignment through oversampling into any standard RL algorithm employing target networks. Third, we provide a formal theoretical analysis demonstrating that learning on aligned transitions accelerates learning efficiency by acting as a variance reduction mechanism. Finally, we support our claims with empirical studies across various discrete and continuous control benchmarks and multiple algorithms, showing that TARK consistently improves performance.

2. Problem statement

We consider a standard Markov decision process (MDP) as usually studied in an RL setting (Sutton & Barto, 1998). We characterize this MDP as a tuple $(\mathcal{S}, \mathcal{A}, P, r, \gamma, p)$, where \mathcal{S} is a finite state space, \mathcal{A} is a finite action space, $P : \mathcal{S} \times \mathcal{A} \rightarrow \Delta(\mathcal{S})$ is a stochastic kernel, $r : \mathcal{S} \times \mathcal{A} \rightarrow \mathbb{R}$ is a reward function, $\gamma \in (0, 1)$ is a discount factor, and $p \in \Delta(\mathcal{S})$ denotes a probability mass function describing the distribution of the initial state, $S_1 \sim p$.

We denote by S_t and A_t the random variables representing the state and action at time t , and by $s \in \mathcal{S}$ and $a \in \mathcal{A}$ their respective realizations. At time step t , the system is in state $S_t \in \mathcal{S}$. If an agent takes action $A_t \in \mathcal{A}$, it receives a corresponding reward $r(s, a)$, and the system transitions to the next state $S_{t+1} \sim P(\cdot | s, a)$. We define the random reward at time t as $R_t = r(S_t, A_t)$. The agent selects actions based on a policy $\pi : \mathcal{S} \rightarrow \mathcal{A}$ via $A_t = \pi(S_t)$. Let $\mathbb{P}_p^\pi(\cdot) = \text{Prob}(\cdot | \pi, S_1 \sim p)$ denote the probability of an event when following a policy π , starting from an initial state $S_1 \sim p$, and let $\mathbb{E}_p^\pi[\cdot]$ denote the corresponding expectation operator. Let n express the number of transitions within the episode. Let G_t denote the discounted return at time t , with

$$G_t = \sum_{i=t}^n \gamma^{i-t} R_i. \quad (2)$$

We define the Q-function (or action-value function) for a policy π as

$$Q^\pi(s, a) = \mathbb{E}_p^\pi [G_t | S_t = s, A_t = a] \quad (3)$$

$$= \mathbb{E}_p^\pi \left[\sum_{i=t}^n \gamma^{i-t} R_i | S_t = s, A_t = a \right]. \quad (4)$$

The ultimate goal of value-based RL is to learn a policy that maximizes the Q-function, leading to $Q^*(s, a) = \max_\pi Q^\pi(s, a)$. The policy is gradually improved by repeatedly interacting with the environment and learning from

previously experienced transitions. A transition C_t is a 5-tuple, $C_t = (S_t, A_t, R_t, S_{t+1}, d_t)$, where d_t is a binary episode termination indicator, $d_t = \mathbb{1}_{t=n}$. One popular approach to learn Q^* is via Watkins’ Q-learning (Watkins (1989); Watkins & Dayan (1992)), where Q-values are gradually updated via

$$Q(S_t, A_t) \leftarrow Q(S_t, A_t) + \eta \cdot \delta_t, \quad (5)$$

with $\eta \in (0, 1]$ being the learning rate and δ_t being the TD error.

In the classical tabular formulation, this TD error is defined using the *online target*,

$$Q_{\text{target}}(S_t) = R_{t+1} + (1 - d_{t+1}) \cdot \gamma \cdot \max_a Q(S_{t+1}, a, \theta), \quad (6)$$

yielding the online TD error

$$\delta_t = Q_{\text{target}}(S_t) - Q(S_t, A_t). \quad (7)$$

In deep RL, and specifically in the DQN algorithm (Mnih et al., 2015), stability is improved by introducing a separate *target network* with parameters $\bar{\theta}$. Crucially, $\bar{\theta}$ is a time-lagged copy of the online parameters θ , such that, under hard updates, $\bar{\theta} \approx \theta_{t-k}$ for some delay k . This target network improves training stability: When a single function approximator is used to both estimate action values and define the bootstrap targets, parameter updates induce correlated changes in predictions and targets, which can lead to divergence. The target network mitigates this issue by decoupling target computation from the online updates, yielding a temporally more stationary learning objective.

The *offline target*—i.e., the target value from the target network, as used in standard DQN—is defined as

$$\bar{Q}_{\text{target}}(S_t) = R_{t+1} + (1 - d_{t+1}) \cdot \gamma \cdot \max_a Q(S_{t+1}, a, \bar{\theta}), \quad (8)$$

which leads to the offline or target TD error

$$\bar{\delta}_t = \bar{Q}_{\text{target}}(S_t) - Q(S_t, A_t). \quad (9)$$

3. Target-Aligned Reinforcement Learning

In this section, we present TARK, a framework designed to mitigate the stability-recency tradeoff in deep RL. We first build the intuition for target alignment by analyzing the interplay between offline and online value estimates. We then formalize this intuition into a computable alignment score. Finally, we introduce an alignment-based oversampling mechanism that integrates this metric into standard off-policy algorithms to prioritize stable *and* recent updates.

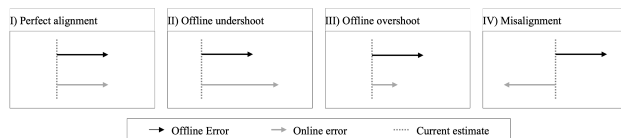


Figure 1. Stylized visualization of alignment scenarios. We distinguish between updates fully supported by the online network (scenario I & II) and updates that are only partially or not at all supported by the online network (scenario III & IV). We posit that update types I and II are safer than update types III and IV.

3.1. Intuition

In contemporary deep RL, value estimates are updated using target values provided by a lagged offline network. While this lag increases stability, it naturally sacrifices recency. TARK resolves this by quantifying the agreement between the stable (offline) target and the most recent (online) estimate. Specifically, it measures the extent to which the update direction and magnitude proposed by the offline target are *supported* by the online network. As displayed in Figure 1, we identify four distinct alignment scenarios.

I) Perfect Alignment. The offline and online updates are identical. The offline target is perfectly aligned with the most recent estimate from the online network.

II) Offline Undershoot. Both networks agree on direction, but the online network proposes a more extreme update. The conservative offline update is therefore *fully supported* by the online view. We treat this as a safe update: the stable target points in the right direction but is simply more cautious than the volatile online network.

III) Offline Overshoot. Both networks agree on direction, but the offline target proposes a more extreme update than the online network. The offline update is therefore only *partially supported*, indicating some level of risk that the frozen offline target overshoots the ideal update magnitude, introducing the potential need for partial update reversion in the future. In essence, the stale target may push the agent too hard, ignoring recent evidence that the value is actually closer than the offline target suggests.

IV) Misalignment. The networks disagree on update direction. The offline target is not at all supported by the current online estimate.

We hypothesize that, all else equal, updates with higher online support are more beneficial for learning. Specifically, we posit that learning is most effective in scenarios I and II, where the recent online target fully supports the stable offline target. Conversely, scenarios III and IV introduce varying degrees of risk. This hypothesis rests on three observations:

Observation 3.1.1 (Avoidance of outdated targets). Misalignment or offline overshoots suggest that the proposed offline update is no longer fully supported by the online

estimate. By performing updates on those targets, we effectively chase targets which are no longer aligned with the most recent information. Avoiding such updates prevents the agent from committing to update steps that have been identified as directionally incorrect or excessively large by the most recent value estimates.

Observation 3.1.2 (Temporal ensembling). The online and offline networks provide complementary estimates of the same value function. While they are temporally reliant, they function as a temporal ensemble. Lower agreement between them may indicate higher epistemic target value uncertainty. Prioritizing alignment then acts as a variance reduction mechanism, filtering updates where the target signal is noisy.

Observation 3.1.3 (Reversion of misaligned changes). Since the target network is periodically updated with online parameters, online target values eventually become the new offline target values. Consequently, updates based on the current offline target that are misaligned with the current online view are likely to be reverted once the target network updates. As such, Q-value updates based on misaligned targets induce oscillatory behavior and are potentially wasteful.

In the following section, we define a metric to formalize the established preference for updates with aligned targets.

3.2. Target Alignment Score

In the following, we formalize the intuition derived in Section 3.1 into a computable *Target Alignment Score* \mathcal{A}_t . This score quantifies, on a per-transition basis, the degree to which the update step proposed by the stable target network is supported by the most recent online estimate. As such, it provides a principled signal for identifying updates that are both stable and up-to-date.

We first define the residual online error δ_t^{next} , which approximates the online error that would remain after applying the update proposed by the offline target,

$$\delta_t^{\text{next}} = \delta_t - \bar{\delta}_t. \quad (10)$$

Using this residual, we define the base alignment score $\mathcal{A}_t^{\text{base}} \in [0, 1]$, which measures the extent to which the offline update reduces the magnitude of the current online error,

$$\mathcal{A}_t^{\text{base}} = \frac{|\delta_t|}{|\delta_t| + |\delta_t^{\text{next}}| + \epsilon}. \quad (11)$$

The denominator $|\delta_t| + |\delta_t^{\text{next}}|$ represents the total variation in error space. If the residual error $|\delta_t^{\text{next}}|$ is small relative to the initial error $|\delta_t|$, base alignment is high. In the ideal scenario where the offline update fully resolves the online error (i.e., $\delta_t^{\text{next}} \rightarrow 0$), the score is maximized (i.e., $\mathcal{A}_t^{\text{base}} \rightarrow 1$). Conversely, if the proposed update exacerbates the error—driving the estimate further from the online target such

that $|\delta_t^{\text{next}}|$ increases—the denominator grows relative to the numerator, diminishing the score towards zero.

However, strict adherence to this base metric would penalize offline over- and undershoots equally. Yet, as established in Section 3.1, in case of an offline undershoot, the designated target is fully supported by the most recent estimate, while it is only partially supported in the offline overshoot case. As such, offline undershoots are safe, whereas offline overshoots may pose risk. To account for this asymmetry, we define the final alignment metric \mathcal{A}_t ,

$$\mathcal{A}_t = \begin{cases} 1 & \text{if } (\delta_t \cdot \bar{\delta}_t > 0) \text{ and } (|\delta_t| > |\bar{\delta}_t|) \\ \mathcal{A}_t^{\text{base}} & \text{else} \end{cases} \quad (12)$$

This metric formally captures our previous intuition: The score equals one in scenarios I and II, where the offline update is fully supported by the online network, and falls below one in scenarios III and IV, reflecting partial or absent online support.

Note on online target stability. The proposed methodology relies on the alignment between online and offline targets. In the broader literature, online targets are often considered too unstable to yield valuable information. However, this instability arises primarily when the online network is used to provide bootstrapped learning targets, as this creates immediate feedback loops. In TARL, the online network is used only for directional validation. As long as the online network is updated based on stable targets provided by the offline network, its estimates remain sufficiently stable to serve as a directional reference for alignment.

3.3. Alignment-based oversampling

We have established the intuition that transitions with high target alignment are more informative for learning than those with low alignment. Building on this insight, we introduce a simple extension to standard RL pipelines that explicitly incorporates target alignment into the learning process to improve sample efficiency.

We introduce *alignment-based oversampling*, which serves as the backbone for TARL: Given a batch size m , we sample $m + b$ where $b \in \mathbb{N}$ transitions from the replay buffer, compute their target alignment \mathcal{A}_t , and select the m transitions with the highest alignment for the update. This mechanism temporarily omits poorly aligned transitions. It effectively acts as a dynamic noise filter, postponing the learning of misaligned transitions until the target network updates and the alignment signal clears up. In consequence, alignment-based oversampling increases batch alignment.

The resulting building block is an easily integrated drop-in refinement that converts any off-policy RL algorithm em-

ploying target networks into its target-aligned version. Algorithm 1 presents an instantiation of Target-Aligned DQN, with the proposed drop-in refinement boxed. Alternative approaches to integrating alignment into existing RL pipelines like prioritized sampling, loss weighting or loss scaling are discussed in Appendix A.

Similar to other established DQN extensions like Double Deep Q-Network (DDQN), TARL requires additional forward passes to compute the target alignment for an enlarged batch. Importantly, the runtime overhead induced by alignment-based oversampling does not scale linearly with b . Given sufficient device memory, these computations may be parallelized and can be executed jointly. As a result, the dominant cost remains a single forward and backward pass through the network, and the marginal cost of TARL is low in practice. This makes alignment-based oversampling a time-efficient extension, even for relatively large oversampling factors, and allows practitioners to trade modest additional computation for substantial gains in sample efficiency.

Moreover, transition prioritization based on alignment offers a distinct advantage over alternative prioritization methods regarding its priority distribution. When the target network is updated under a hard update regime, it is overwritten with the current online network. Consequently, target alignment is maximized for each transition. As learning progresses, updates induce changes in value estimates. As alignment was maximized initially, estimate changes may only decrease alignment, leading to overall alignment decay. We expect that value estimate changes are larger for sampled transitions than for unsampled transitions, as the former are modulated directly. In consequence, alignment decays faster for sampled transitions. Thus, when alignment is used as a transition selection criterion, it induces an implicit form of batch stratification. Therefore, in contrast to other prioritization schemes, which can violate the i.i.d. assumption, alignment-based prioritization can naturally counteract this phenomenon.

4. Theoretical Analyses

While classical convergence results for deep Q-learning often rely on asymptotic arguments as the number of updates tends to infinity, our focus in this work is on the *efficiency and stability* of the learning trajectory. To quantify this stability, we first introduce a geometric framework for analyzing the consistency of update vectors over time.

4.1. Framework

Our theoretical argument for the effectiveness of TARL relies on two central hypotheses that build upon the idea of directional consistency.

Algorithm 1 Target-Aligned Deep Q-Network (TA-DQN)

Input: Replay buffer \mathcal{D} , discount factor γ , batch size m , oversampling size b , target update frequency C , budget T
 Initialize $Q(s, a; \theta)$ with parameters θ
 Initialize $Q'(s, a; \bar{\theta})$ with parameters $\bar{\theta} \leftarrow \theta$
 Initialize $\mathcal{D} \leftarrow \emptyset$
 Sample initial state $S_1 \sim p$
for $t = 1, \dots, T$ **do**
 Select action A_t using ϵ -greedy policy w.r.t. $Q(S_t, \cdot; \theta)$
 Execute A_t , observe reward R_t and next state S_{t+1}
 Store transition $C_t = (S_t, A_t, R_t, S_{t+1}, d_t)$ in \mathcal{D}

Sample random oversized minibatch $\{M_j\}_{j=1}^{m+b}$ from \mathcal{D}
 Compute alignment metric \mathcal{A}_j for M_j
 Obtain final minibatch $\mathcal{C} \leftarrow \text{TopK}_m(M, \mathcal{A})$

 for $(S_j, A_j, R_j, S_{j+1}, d_j) \in \mathcal{C}$ **do**
 Compute target,
 $y_j = R_j + d_j \gamma \max_{a'} Q'(S_{j+1}, a'; \bar{\theta})$
 end for
 Update θ by minimizing loss,
 $L(\theta) = \frac{1}{m} \sum_{j=1}^m (y_j - Q(S_j, A_j; \theta))^2$
 if $t \pmod{C} = 0$ **then**
 Update target network: $\bar{\theta} \leftarrow \theta$
 end if
end for

Directional consistency. Consider parameter updates of the form $\theta^{(k+1)} = \theta^{(k)} - \eta^{(k)} g^{(k)}$, where $g^{(k)}$ denotes the stochastic update direction induced by the current target network. Let K denote the target update period. We say that updates exhibit *directional consistency* if successive update directions $g^{(k)}$ and $g^{(k+K)}$ —stemming from the same transition but different target networks—are aligned.

Based on this notion, we introduce the *Efficiency Hypothesis* (4.1.1) and the *Proxy Hypothesis* (4.1.2).

Hypothesis 4.1.1 (Efficiency Hypothesis). The effective progress of the algorithm is governed by the consistency of update directions induced by successive target networks. Misalignment between update directions at iterations k and $k + K$ acts as a source of variance, causing oscillations in parameter space that hinder progress. Conversely, increased directional consistency reduces this variance, leading to more stable and efficient learning.

Hypothesis 4.1.2 (Proxy Hypothesis). For intermediate times $k+t$ ($0 < t < K$), the online network $\theta^{(k+t)}$ captures valid local gradient information. Since the online network has digested recent experiences that the target network has not yet seen, the online network acts as a noisy preview of the future target network $\theta^{(k+K)}$: Previous updates within the same target update interval serve as a proxy for the update direction towards the eventual fixed point at the end of

the interval, $\theta^{(k+K)}$.

Implications. Consequently, if alignment between current and future targets leads to more stable learning, and if we may approximate future targets using the online target, the alignment between the current offline target and the online target captures valuable information to stabilize the learning process. In the remainder of this section, we present a formal argument for Hypothesis 4.1.1 and 4.1.2 using a simplified analysis of update productivity.

4.2. Consistency and Update Efficiency

To formalize the link between directional consistency and learning speed, we analyze a simplified model of update productivity. Let θ^* be the optimal policy parameters, let θ denote the current policy parameters, and let θ' denote the future policy parameters after some designated update step. We define a *productive update* as one that reduces the parameter error $|\theta' - \theta^*| < |\theta - \theta^*|$, and an *unproductive update* as one that increases it or stalls progress. Let λ denote the baseline probability that an update is productive. For a learning agent, λ satisfies $\lambda > 0.5$. We assume that the magnitude of updates is independent of its productivity, such that the probability of productivity serves as a valid proxy for expected convergence speed.

In practice, θ^* is unknown. However, we subsequently show that the temporal consistency of update propositions for the same transition conveys information on update productivity. We first establish that for any learning agent, successive updates are naturally positively correlated.

Let $U_t^{(k)}$ and $U_t^{(k+K)}$ be the update steps proposed for transition t by the target network at step k and the future target network at step $k + K$, respectively.

Lemma 4.2.1 (Nonnegative Alignment). *Let updates be productive with probability $\lambda > 0.5$. If $U_t^{(k)}$ and $U_t^{(k+K)}$ are treated as samples from this distribution, the probability of them agreeing on direction (alignment) is strictly greater than random chance:*

$$P(\text{Aligned}) = \lambda^2 + (1 - \lambda)^2 \geq 0.5. \quad (13)$$

Consequently, the sign correlation c between successive updates is non-negative ($c \geq 0$).

For a formal justification, we refer to Appendix B.1.

Building on this, we show that filtering for alignment amplifies convergence speed.

Lemma 4.2.2 (Consistency-Driven Acceleration). *Given a baseline productivity $\lambda > 0.5$ and a non-negative update correlation $c \geq 0$, restricting updates to aligned transitions increases the expected convergence speed p beyond*

the baseline λ :

$$p = P(\text{Productive} \mid \text{Aligned}) > \lambda. \quad (14)$$

Conversely, updates where signs disagree are productive with probability 0.5, leading to stagnation.

Proof Sketch. Using Bayes' Theorem, the probability that an update is productive given that it aligns with the future update is

$$p = \frac{\lambda^2 + c\lambda(1 - \lambda)}{\lambda^2 + (1 - \lambda)^2 + 2c\lambda(1 - \lambda)}. \quad (15)$$

For any $c \in [0, 1]$ and $\lambda > 0.5$, this ratio strictly exceeds λ . In contrast, misaligned updates imply one step is towards θ^* and one is away, averaging to zero progress. Thus, filtering for consistency strictly improves the expected signal-to-noise ratio of the update stream. \square

For the complete proof, we refer to Appendix B.2.

This result suggests that global convergence speed can be accelerated by prioritizing aligned updates and deferring misaligned ones, effectively lowering the variance of the optimization trajectory.

4.3. Latent Alignment via Online Approximation

While the previous analysis relied on comparing current and future updates, the future target at step $k + K$ is not observable at step $k + i$, where $0 < i < K$. We thus provide a formal argument that we may obtain an informative proxy for future consistency using online information.

We define the *Latent Temporal Alignment* \bar{A}_t as the ideal consistency metric between the current offline error $\bar{\delta}_t$, updated at step k , and the future offline error $\bar{\delta}'_t$ at step $k + K$. A theoretically optimal algorithm would preferentially sample transitions where \bar{A}_t is high, indicating the current update is supported by the future target.

Since $\bar{\delta}'_t$ is unknown, TARTL substitutes it with the current online error δ_t . This substitution rests on the property that the online network, having absorbed recent gradients, acts as a leading indicator for the future target network.

Assumption 4.3.1 (Online Approximation). We presume learning under a sufficiently small learning rate η . Let i denote the current timestep. Then, the aggregated stochastic gradient for the updates in $[k, k + i]$ is a better-than-random estimate of the stochastic gradient obtained in its superset, the updates in $[k, k + K]$.

This implies that δ is a superior estimator of $\bar{\delta}'$ than $\bar{\delta}$,

$$\|\delta - \bar{\delta}'\|_\mu^2 \leq \|\bar{\delta} - \bar{\delta}'\|_\mu^2. \quad (16)$$

Theorem 4.3.2 (Alignment Approximation Bound). *Let \mathcal{A}_t denote the TARL alignment score (using δ_t as a proxy) and $\mathcal{A}_t^{\text{naive}} \equiv 1$ denote the implicit alignment score of standard RL (which does not control for alignment and thereby implicitly assumes uniformly perfect alignment). Let ϵ_{TARL} and ϵ_{naive} be the absolute errors of these metrics with respect to the true Latent Alignment $\bar{\mathcal{A}}_t$. Under Assumption 4.3.1, it holds that*

$$\epsilon_{\text{TARL}} \leq \epsilon_{\text{naive}}. \quad (17)$$

In essence, because the online network is statistically closer to the future target than the current target is, TARL provides a more accurate lower-bound on the true alignment score than established methods, which blindly assume uniform perfect alignment.

Proof Sketch. Let $f : \mathbb{R} \rightarrow [0, 1]$ be a monotone alignment scoring function that saturates at 1 for inputs exceeding the offline threshold $\bar{\delta}_t$. The naive baseline always assigns score 1, while TARL evaluates the score using the online update magnitude δ_t .

If the online and offline updates agree ($\delta_t \geq \bar{\delta}_t$), both methods output one. Otherwise ($0 \leq \delta_t < \bar{\delta}_t$), the scoring function reduces to a linear map over this interval. Under Assumption 4.3.1, the online estimate used by TARL is strictly closer to the future estimate than the naive offline baseline. The linear map preserves this ordering. Hence, TARL achieves an equal or tighter approximation error in all cases. \square

For the complete proof, we refer to Appendix B.3.

Conclusion. Our theoretical analysis formalizes the intuition behind TARL. First, directional consistency serves as a necessary condition for efficient learning (Section 4.2). Second, while the future target estimate is unobservable, the instantaneous online estimate serves as a reliable proxy (Section 4.3). By filtering updates where the online proxy contradicts the offline target, TARL effectively omits transitions destined for future update reversal, thereby stabilizing the training dynamics.

5. Numerical results

We evaluate TARL across both continuous and discrete control domains to assess its generality. Our experimental design is chosen to test the hypothesis that target alignment is a fundamental principle, agnostic to the specific target update mechanism. We test this hypothesis in discrete control environments using DQN, as well as in continuous control environments using SAC. We run three experiments.

1. *Discrete control with hard updates.* We evaluate the effectiveness of TARL on MINATAR (Young & Tian,

2019) environments using classic DQN, which employs hard target updates.

2. *Continuous Control with soft updates.* We evaluate TARL on MUJoCo (Todorov et al., 2012) environments using SAC, which relies on soft target updates.
3. *Ablations.* We provide ablations, in which we further investigate the impacts of soft and hard target update regimes within the same algorithm, and evaluate the compatibility of TARL with the DDQN target.

This selection allows us to test performance across substantially different learning dynamics, action modalities, target value formulations and target network update regimes.

Crucially, we performed no hyperparameter tuning for TARL. We applied TARL as a direct drop-in refinement without re-tuning the base hyperparameters of the original algorithms. We also did not tune the TARL-specific oversampling hyperparameter b , but statically set $b = m$. This design choice aims to show the flexibility and robustness of TARL, and highlights its ease of integration into existing pipelines. Nonetheless, explicit hyperparameter tuning may further increase performance. For additional details on our experimental setting, we refer to Appendix C.

Discrete control with hard updates. We compared DQN performance with and without TARL along four different MINATAR environments, namely ASTERIX, BREAKOUT, FREEWAY and SPACEINVADERS. For each environment, we recorded performance within five seeds. We find that Target-aligned DQN consistently achieved faster convergence and higher performance than DQN across all four environments, as shown in Figure 2. This effect is extremely robust: It does not only show on average across seeds, but also in every single seed individually, as shown in Appendix D, Figure 5. This finding suggests that when targets are frozen for prolonged intervals, filtering out misaligned transitions during the frozen period significantly improves training dynamics.

Continuous Control with soft updates. We compared SAC performance with and without TARL along six different MUJoCo environments, namely HALFCHEETAH, ANT, HOPPER, WALKER2D, SWIMMER, and HUMANOID. For each environment, we recorded performance within five seeds. As displayed in Figure 3, we observed that Target-aligned SAC achieved faster convergence and higher performance than SAC in five out of six environments. This finding is also very robust across individual seeds, as shown in Appendix D, Figure 6. The gains in this regime highlight that even within modern algorithms under soft updates, explicit alignment filtering improves training dynamics.

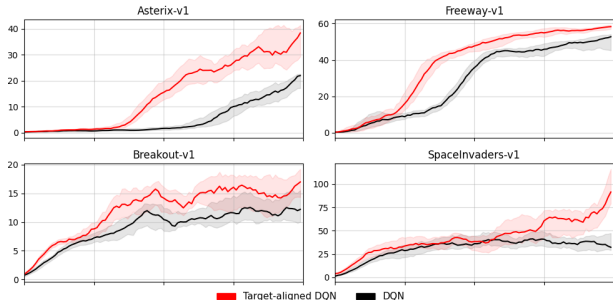


Figure 2. Performance comparison between DQN and target-aligned DQN on four games of the MINATAR benchmark over five seeds. Curves represent median returns, smoothed over 10 points, and shaded areas indicate interquartile ranges.

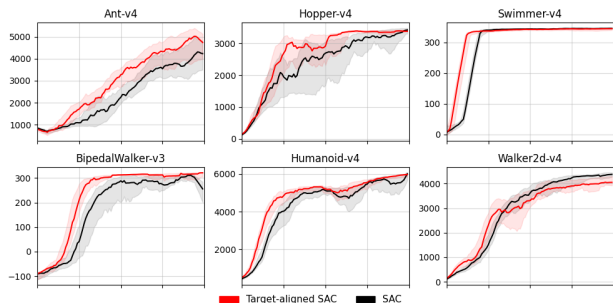


Figure 3. Performance comparison between SAC and target-aligned SAC on six games of the MUJoCo benchmarks over five seeds. Curves represent median returns, smoothed over 10 points, and shaded areas indicate interquartile ranges.

Ablations. We further ran experiments for the classic DDQN employing both hard and soft updates ($\tau = 0.01$) using the previously established MINATAR setup. This ablation aims to test the impact of soft and hard updates and their compatibility with TARL within the same algorithm, while simultaneously verifying the compatibility with DDQN’s distinct target value formulation (van Hasselt et al., 2015).

As displayed in Figure 4, we find that TARL consistently improves performance of the DDQN. We further find that TARL improves learning dynamics under both soft and hard update regimes, and find no indication of a systematic difference in TARL-induced benefit between them.

6. Discussion

Across a diverse set of environments, for multiple algorithms, and under both hard and soft target network update regimes, algorithms employing TARL consistently outperform their counterparts without alignment correction. Importantly, these improvements are achieved without any additional hyperparameter tuning, highlighting the robustness of the proposed approach. Moreover, TARL can be seamlessly integrated into existing RL pipelines, making

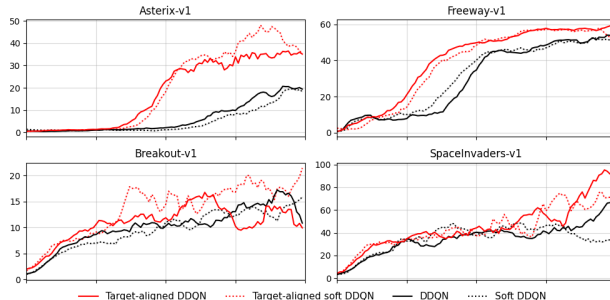


Figure 4. Performance comparison between DDQN and target-aligned DDQN on four games of the MINATAR benchmark. Curves represent median returns, smoothed over 10 points,

it a practical drop-in enhancement that reliably improves performance.

While increasing performance, TARL also incurs some computational overhead. Similar to other established DQN extensions like DDQN, TARL increases the number of required forward passes during training. However, the resulting increase in wall-clock training time is modest in practice, as forward passes are highly parallelizable and can be executed efficiently within modern RL frameworks. We argue that the slight increase in computational cost is outweighed by the significant enhancement of learning dynamics.

7. Conclusion

We introduced TARL, a method that prioritizes updates on transitions with high target alignment between offline and online targets. Central to our approach is a novel alignment metric that quantifies the consistency between update targets across target network updates. By leveraging this metric as a transition selection criterion, TARL ensures target recency and stability. TARL thereby circumvents the stability-recency tradeoff induced by target networks.

Our theoretical analysis demonstrates that TARL increases convergence speed. Empirical evaluation across a variety of benchmarks and algorithms further validates TARL’s effectiveness.

TARL can be seamlessly integrated into existing RL pipelines without requiring additional hyperparameter tuning. Beyond the immediate practical benefits, our work highlights that the online network—despite being too unstable to serve reliable target values—holds valuable information for directional update validation. We are optimistic that TARL will inspire further research into enhancing sample efficiency and overall performance of state-of-the-art RL algorithms. Future directions include the design of alignment-aware loss functions and the exploration of alternative uses of alignment signals within RL.

Impact Statement

This work advances the foundations of reinforcement learning by improving training stability and sample efficiency. By enabling faster and more reliable learning, the proposed method may lower barriers to applying reinforcement learning in real-world domains such as robotics, control, and resource management.

References

- Badia, A. P., Piot, B., Kapturowski, S., Sprechmann, P., Vitvitskyi, A., Guo, D., and Blundell, C. Agent57: Outperforming the Atari Human Benchmark, 2020. URL <https://arxiv.org/abs/2003.13350>.
- Chen, L., Lu, K., Rajeswaran, A., Lee, K., Grover, A., Laskin, M., Abbeel, P., Srinivas, A., and Mordatch, I. Decision transformer: Reinforcement learning via sequence modeling, 2021. URL <https://arxiv.org/abs/2106.01345>.
- Elsayed, M., Vasan, G., and Mahmood, A. R. Deep reinforcement learning without experience replay, target networks, or batch updates. In *NeurIPS 2024 Workshop on Fine-Tuning in Modern Machine Learning: Principles and Scalability*, 2024. URL <https://openreview.net/forum?id=yqQJGTDGXN>.
- Fujimoto, S., van Hoof, H., and Meger, D. Addressing function approximation error in actor-critic methods, 2018. URL <https://arxiv.org/abs/1802.09477>.
- Haarnoja, T., Zhou, A., Abbeel, P., and Levine, S. Soft Actor-Critic: Off-Policy Maximum Entropy Deep Reinforcement Learning with a Stochastic Actor, 2018. URL <https://arxiv.org/abs/1801.01290>.
- Hessel, M., Modayil, J., van Hasselt, H., Schaul, T., Ostrovski, G., Dabney, W., Horgan, D., Piot, B., Azar, M., and Silver, D. Rainbow: Combining Improvements in Deep Reinforcement Learning, 2017. URL <https://arxiv.org/abs/1710.02298>.
- Kim, S., Asadi, K., Littman, M., and Konidaris, G. Deepmellow: Removing the need for a target network in deep q-learning. In *Proceedings of the Twenty-Eighth International Joint Conference on Artificial Intelligence, IJCAI-19*, pp. 2733–2739. International Joint Conferences on Artificial Intelligence Organization, 7 2019. doi: 10.24963/ijcai.2019/379. URL <https://doi.org/10.24963/ijcai.2019/379>.
- Kobayashi, T. and Ilboudo, W. E. L. t-soft update of target network for deep reinforcement learning. *Neural Networks*, 136:63–71, 2021. ISSN 0893-6080. doi: <https://doi.org/10.1016/j.neunet.2020.12.023>. URL <https://www.sciencedirect.com/science/article/pii/S0893608020304482>.
- Li, S. E. *Deep Reinforcement Learning*, pp. 365–402. Springer Nature Singapore, Singapore, 2023. ISBN 978-981-19-7784-8. doi: 10.1007/978-981-19-7784-8_10. URL https://doi.org/10.1007/978-981-19-7784-8_10.
- Lillicrap, T. P., Hunt, J. J., Pritzel, A., Heess, N., Erez, T., Tassa, Y., Silver, D., and Wierstra, D. Continuous control with deep reinforcement learning, 2015. URL <https://arxiv.org/abs/1509.02971>.
- Mnih, V., Kavukcuoglu, K., Silver, D., Rusu, A. A., Veness, J., Bellemare, M. G., Graves, A., Riedmiller, M., Fidjeland, A. K., Ostrovski, G., Petersen, S., Beattie, C., Sadik, A., Antonoglou, I., King, H., Kumaran, D., Wierstra, D., Legg, S., and Hassabis, D. Human-level control through deep reinforcement learning. *Nature*, 518(7540):529–533, February 2015. ISSN 0028-0836, 1476-4687. doi: 10.1038/nature14236. URL <https://www.nature.com/articles/nature14236>.
- Piché, A., Thomas, V., Pardinas, R., Marino, J., Marconi, G. M., Pal, C., and Khan, M. E. Bridging the gap between target networks and functional regularization, 2023. URL <https://arxiv.org/abs/2106.02613>.
- Polyak, B. T. and Juditsky, A. B. Acceleration of stochastic approximation by averaging. *SIAM Journal on Control and Optimization*, 30(4):838–855, 1992. doi: 10.1137/0330046. URL <https://doi.org/10.1137/0330046>.
- Raffin, A. RL baselines3 zoo. <https://github.com/DLR-RM/rl-baselines3-zoo>, 2020.
- Schaul, T., Quan, J., Antonoglou, I., and Silver, D. Prioritized Experience Replay. 2015. doi: 10.48550/ARXIV.1511.05952. URL <https://arxiv.org/abs/1511.05952>.
- Schwarzer, M., Obando-Ceron, J., Courville, A., Bellemare, M., Agarwal, R., and Castro, P. S. Bigger, Better, Faster: Human-level Atari with human-level efficiency, 2023. URL <https://arxiv.org/abs/2305.19452>.
- Sutton, R. Learning to predict by the method of temporal differences. *Machine Learning*, 3:9–44, 08 1988. doi: 10.1007/BF00115009.
- Sutton, R. and Barto, A. Reinforcement Learning: An Introduction. *IEEE Transactions on Neural Networks*, 9(5):1054–1054, September 1998. ISSN 1045-9227, 1941-0093. doi: 10.1109/TNN.1998.712192. URL <https://ieeexplore.ieee.org/document/712192/>.

- Todorov, E., Erez, T., and Tassa, Y. Mujoco: A physics engine for model-based control. In *2012 IEEE/RSJ International Conference on Intelligent Robots and Systems*, pp. 5026–5033, 2012. doi: 10.1109/IROS.2012.6386109.
- van Hasselt, H., Guez, A., and Silver, D. Deep Reinforcement Learning with Double Q-learning, 2015. URL <https://arxiv.org/abs/1509.06461>.
- Vincent, T., Tripathi, Y., Faust, T., Oren, Y., Peters, J., and D’Eramo, C. Bridging the performance gap between target-free and target-based reinforcement learning, 2025. URL <https://arxiv.org/abs/2506.04398>.
- Watkins, C. *Learning From Delayed Rewards*. PhD thesis, Kings College, London, 1989.
- Watkins, C. J. C. H. and Dayan, P. Q-learning. *Machine Learning*, 8(3-4):279–292, May 1992. ISSN 0885-6125, 1573-0565. doi: 10.1007/BF00992698. URL <http://link.springer.com/10.1007/BF00992698>.
- Young, K. and Tian, T. Minatar: An atari-inspired testbed for thorough and reproducible reinforcement learning experiments, 2019. URL <https://arxiv.org/abs/1903.03176>.
- Zhang, H., Bai, F., Xiao, C., Gao, C., Xu, B., and Müller, M. Beta-dqn: Improving deep q-learning by evolving the behavior, 10 2025.
- Zhang, S., Yao, H., and Whiteson, S. Breaking the deadly triad with a target network. In Meila, M. and Zhang, T. (eds.), *Proceedings of the 38th International Conference on Machine Learning*, volume 139 of *Proceedings of Machine Learning Research*, pp. 12621–12631. PMLR, 18–24 Jul 2021. URL <https://proceedings.mlr.press/v139/zhang21y.html>.

A. Alternative approaches

Several alternatives to oversampling are worth considering to integrate alignment into the learning process:

Prioritized sampling. Replay transitions could be sampled based on alignment, favoring well-aligned updates. However, this would require computing alignment for the full buffer, which is computationally prohibitive. Approximate solutions, such as maintaining stored alignment values updated on sampling (analogous to Prioritized Experience Replay (Schaul et al., 2015)), are likely not applicable, as the alignment metric relies on frequently changing online estimates.

Loss weighting. Alignment can be used as a weight within the loss function, upweighting well-aligned samples and downweighting poorly aligned ones. While flexible, this approach requires hyperparameter tuning and may interfere with other loss-weighting schemes (e.g., importance sampling in PER), thereby limiting the method’s general applicability.

Loss scaling. Alternatively, alignment may be used to directly scale the loss, effectively modulating the learning rate on a per-sample basis. This is conceptually clean but risks destabilization unless normalization or re-scaling strategies are applied, requiring careful hyperparameter tuning.

We consider oversampling the most robust and conceptually sound approach, as it does not require hyperparameter tuning, is easily integrated into existing pipelines and ensures target alignment while causing limited computational overhead. We therefore deliberately chose to limit this paper’s scope to oversampling. Yet, we plan to pursue different variants of alignment integration in future work.

B. Theoretical Proofs

In this section, we provide the full derivations for the Lemmas and Theorems presented in Section 4. To ensure rigor, we explicitly formalize the probability spaces and the simplifying assumptions used to model the update dynamics.

B.1. Derivation 4.1: The Correlated Update Model

Note: Rather than proving alignment from first principles, we herein formalize the probabilistic model used to justify the hypothesis of non-negative alignment, formalized in Lemma 4.2.1.

Let \mathcal{U} denote the space of all update propositions generated during training, partitioned into productive ($\mathcal{U}^{(+)}$) and unproductive ($\mathcal{U}^{(-)}$) subsets. We define the baseline productivity λ as the probability of a random update being correct:

$$\lambda := P(U \in \mathcal{U}^{(+)}) = \frac{|\mathcal{U}^{(+)}|}{|\mathcal{U}^{(+)}| + |\mathcal{U}^{(-)}|} > 0.5. \quad (18)$$

Consider two update propositions $U^{(k)}$ and $U^{(k+K)}$ for the same transition, generated by target networks at steps k and $k + K$. We model these as binary random variables $X, Y \in \{-1, 1\}$, where values match the sign of the optimal update (1 for productive, -1 for unproductive).

Baseline (Independence): If X and Y were independent samples from \mathcal{U} , the probability of them agreeing on direction (alignment) would be solely a function of the bias λ :

$$P_{\text{indep}}(X = Y) = \underbrace{\lambda^2}_{\text{Both Prod.}} + \underbrace{(1 - \lambda)^2}_{\text{Both Unprod.}} \geq 0.5. \quad (19)$$

Strict inequality holds for $\lambda > 0.5$.

The Correlated Model: In practice, X and Y are derived from the *same* state-transition tuple (s, a, r, s') . This shared ground truth introduces a temporal dependency. We argue that independence serves as a conservative lower bound: the shared structure implies that target networks are strictly more likely to agree than if they were statistically independent.

$$P_{\text{real}}(X = Y) \geq P_{\text{indep}}(X = Y).$$

We model this excess agreement via a correlation coefficient c :

$$P_{\text{real}}(X = Y) = \lambda^2 + (1 - \lambda)^2 + 2c\lambda(1 - \lambda). \quad (20)$$

Comparing the real and independent cases implies that the correlation term must be non-negative:

$$2c\lambda(1 - \lambda) \geq 0 \implies c \geq 0.$$

This derivation justifies the use of a non-negative correlation parameter $c \in [0, 1)$ in the subsequent analysis of convergence speed.

B.2. Proof of Lemma 4.2: Consistency-Driven Acceleration

Lemma 4.2. Given a baseline productivity $\lambda > 0.5$ and a non-negative update correlation $c \geq 0$, restricting updates to aligned transitions increases the expected convergence speed p beyond the baseline λ :

$$p = P(\text{Productive} \mid \text{Aligned}) > \lambda.$$

Proof. We adopt the *Bounded Magnitude Assumption*: We assume that the magnitude of updates is independent of their sign correctness, such that the probability of productivity serves as a valid proxy for expected convergence speed.

We aim to calculate the conditional probability $p = P(X = S^* \mid X = Y)$. Using the joint probabilities derived in the Proof of Lemma 4.1, and letting c represent the normalized covariance term such that the joint success probability is $\lambda^2 + c\lambda(1 - \lambda)$:

$$\begin{aligned} p &= \frac{P(X = S^* \cap X = Y)}{P(X = Y)} \\ &= \frac{P(X = S^*, Y = S^*)}{P(X = S^*, Y = S^*) + P(X \neq S^*, Y \neq S^*)} \\ &= \frac{\lambda^2 + c\lambda(1 - \lambda)}{\lambda^2 + (1 - \lambda)^2 + 2c\lambda(1 - \lambda)}. \end{aligned}$$

We define the function $g(c)$ for a fixed $\lambda > 0.5$:

$$g(c) = \frac{\lambda^2 + c\gamma}{\lambda^2 + (1 - \lambda)^2 + 2c\gamma}, \quad \text{where } \gamma = \lambda(1 - \lambda) > 0.$$

To prove $g(c) > \lambda$, we analyze the inequality directly.

$$\begin{aligned} \frac{\lambda^2 + c\gamma}{\lambda^2 + (1 - \lambda)^2 + 2c\gamma} &> \lambda \\ \lambda^2 + c\gamma &> \lambda [\lambda^2 + (1 - \lambda)^2 + 2c\gamma] \quad (\text{since denominator} > 0) \\ \lambda^2 + c\gamma &> \lambda^3 + \lambda(1 - \lambda)^2 + 2c\lambda\gamma \\ c\gamma - 2c\lambda\gamma &> \lambda^3 + \lambda(1 - 2\lambda + \lambda^2) - \lambda^2 \\ c\gamma(1 - 2\lambda) &> \lambda^3 + \lambda - 2\lambda^2 + \lambda^3 - \lambda^2 \\ c\gamma(1 - 2\lambda) &> 2\lambda^3 - 3\lambda^2 + \lambda \\ c\lambda(1 - \lambda)(1 - 2\lambda) &> \lambda(2\lambda^2 - 3\lambda + 1). \end{aligned}$$

Factorizing the quadratic term $2\lambda^2 - 3\lambda + 1$:

$$2\lambda^2 - 3\lambda + 1 = (2\lambda - 1)(\lambda - 1).$$

Substituting this back:

$$c\lambda(1 - \lambda)(1 - 2\lambda) > \lambda(2\lambda - 1)(\lambda - 1).$$

Dividing both sides by λ (since $\lambda > 0$):

$$c(1 - \lambda)(1 - 2\lambda) > (2\lambda - 1)(\lambda - 1).$$

Note that $(\lambda - 1) = -(1 - \lambda)$ and $(2\lambda - 1) = -(1 - 2\lambda)$. Thus the RHS becomes:

$$(2\lambda - 1)(\lambda - 1) = [-(1 - 2\lambda)][-(1 - \lambda)] = (1 - 2\lambda)(1 - \lambda).$$

The inequality simplifies to:

$$c(1 - \lambda)(1 - 2\lambda) > (1 - \lambda)(1 - 2\lambda).$$

We divide by $(1 - \lambda)$, which is positive since $\lambda < 1$:

$$c(1 - 2\lambda) > (1 - 2\lambda).$$

Dividing both sides by $\lambda(1 - \lambda)$ (where $1 - \lambda = -(\lambda - 1)$):

$$c(1 - 2\lambda) > -(2\lambda - 1) = 1 - 2\lambda.$$

Finally, we divide by $(1 - 2\lambda)$. Since $\lambda > 0.5$, the term $(1 - 2\lambda)$ is *negative*. Dividing by a negative number flips the inequality:

$$c < 1.$$

Thus, this condition holds for all non-negative $c < 1$, that is, per Section B.1, for every converging model with imperfect alignment. This result implies that the alignment filter is most effective when errors are independent ($c = 0$) or imperfectly correlated. As the correlation approaches identity ($c \rightarrow 1$), the information gain from alignment vanishes, and $p \rightarrow \lambda$. Since deep RL updates typically exhibit imperfect correlation ($c < 1$) due to network lag and mini-batch noise, the alignment filter theoretically accelerates convergence.

Thus, the condition $p > \lambda$ holds true for any $c < 1$. In the simplified case of $c = 0$ (independent updates), the boost is substantial. As correlation approaches 1 ($c \rightarrow 1$), the benefit diminishes ($p \rightarrow \lambda$) but never becomes negative. □

B.3. Proof of Theorem 4.3: Alignment Approximation Bound

Theorem 4.3. Let $\epsilon_{\text{TARL}} = |\bar{\mathcal{A}}_t - \mathcal{A}_t|$ denote the approximation error of the *TARL* alignment metric, and $\epsilon_{\text{naive}} = |\bar{\mathcal{A}}_t - \mathcal{A}_t^{\text{naive}}|$ denote the error of the standard baseline. Under Assumption 4.2 (that the online error δ_t is a better estimator of the future error $\bar{\delta}'_t$ than the offline error $\bar{\delta}_t$), it holds that $\epsilon_{\text{TARL}} \leq \epsilon_{\text{naive}}$.

Proof. Let $f(x) : \mathbb{R} \rightarrow [0, 1]$ be the alignment scoring function defined in Eq. 12. Without loss of generality, assume $\bar{\delta}_t > 0$. The function is defined such that $f(x) = 1$ for $x \geq \bar{\delta}_t$, and $f(x)$ is strictly monotonically increasing for $x \in [0, \bar{\delta}_t]$.

We compare the errors of the two estimators against the true latent score $\bar{\mathcal{A}}_t = f(\bar{\delta}'_t)$:

- *Naive Baseline:* $\mathcal{A}^{\text{naive}} = f(\bar{\delta}_t) = 1$.
- *TARL Estimator:* $\mathcal{A}_t = f(\delta_t)$.

Case 1: Consistency ($\delta_t \geq \bar{\delta}_t$). Here, the online update magnitude confirms the offline update. Since $\delta_t \geq \bar{\delta}_t$, we have $f(\delta_t) = 1$. Both estimators yield 1, so $\epsilon_{\text{TARL}} = \epsilon_{\text{naive}} = 0$.

Case 2: Disagreement ($0 \leq \delta_t < \bar{\delta}_t$). Here, the online network suggests the offline target overshoots. The *TARL* score adapts: $\mathcal{A}_t = f(\delta_t)$.

First, we establish the explicit form of the metric in this domain. Recall Eq. (8):

$$f(x) = \frac{|x|}{|x| + |x - \bar{\delta}_t|}.$$

Since $0 \leq x < \bar{\delta}_t$, the terms simplify to $|x| = x$ and $|x - \bar{\delta}_t| = \bar{\delta}_t - x$. The denominator becomes constant: $x + (\bar{\delta}_t - x) = \bar{\delta}_t$. Thus, the metric acts as a linear scaler: $f(x) = x/\bar{\delta}_t$. Linearity implies that distance in score space is proportional to distance in error space:

$$|f(a) - f(b)| = \frac{1}{\bar{\delta}_t} |a - b|.$$

We now use this property to evaluate the approximation errors. For the Naive baseline (which estimates $1 = f(\bar{\delta}_t)$):

$$\epsilon_{\text{naive}} = |1 - \bar{\mathcal{A}}_t| = |f(\bar{\delta}_t) - f(\bar{\delta}'_t)| = \frac{1}{\bar{\delta}_t} |\bar{\delta}_t - \bar{\delta}'_t|.$$

For T_{ARL} (which estimates $f(\delta_t)$):

$$\epsilon_{\text{TARL}} = |f(\delta_t) - \bar{\mathcal{A}}_t| = |f(\delta_t) - f(\bar{\delta}'_t)| = \frac{1}{\delta_t} |\delta_t - \bar{\delta}'_t|.$$

We now compare the two errors. Assumption 4.2 states that the online error is spatially closer to the future error than the offline error is:

$$|\delta_t - \bar{\delta}'_t| \leq |\bar{\delta}_t - \bar{\delta}'_t|.$$

Multiplying this inequality by the positive constant $\frac{1}{\delta_t}$ and substituting the definitions above directly yields:

$$\epsilon_{\text{TARL}} \leq \epsilon_{\text{naive}}.$$

Thus, T_{ARL} provides a strictly tighter (or equal) bound on the true alignment score. □

C. Hyperparameters

Hyperparameters for SAC were set to the MuJoCo standard defined in the RL Baselines3 Zoo (Raffin, 2020). In HALFCHEETAH, ANT, HOPPER, WALKER2D, and SWIMMER, we trained for 1 million timesteps per run. In HUMANOID, we trained for 2 million timesteps per run.

Table 1. Hyperparameters for SAC in MuJoCo.

PARAMETER	VALUE
LEARNING RATE	$3e - 4$
BUFFER SIZE	$1e6$
BATCH SIZE	256
LEARNING STARTS	$1e4$
DISCOUNT FACTOR	0.99^1
SOFT UPDATE COEFFICIENT	0.005
UPDATE PER STEPS	1
# GRADIENT STEPS	1

DQN hyperparameters for MINATAR were set to recommendations published within Zhang et al. (2025). We trained for 2 million timesteps per run.

Table 2. Hyperparameters for DQN in MinAtar.

PARAMETER	VALUE
LEARNING RATE	$2.5e - 4$
BUFFER SIZE	$1e5$
BATCH SIZE	32
LEARNING STARTS	$5,000$
DISCOUNT FACTOR	0.99
TARGET UPDATE INTERVAL	$1,000$
STARTING EXPLORATION	1.0
EXPLORATION FRACTION	0.05
FINAL EXPLORATION	0.01

Evaluation. For all environments, 100 evaluations were evenly spaced throughout the training procedure. Each agent evaluation consisted of five full trajectories in the environment, going from initial to terminal state. The evaluation score of a single agent evaluation is the average total score across those five evaluation trajectories.

¹In Swimmer-v4, a decay factor of 0.999 was used.

D. Seed-specific results

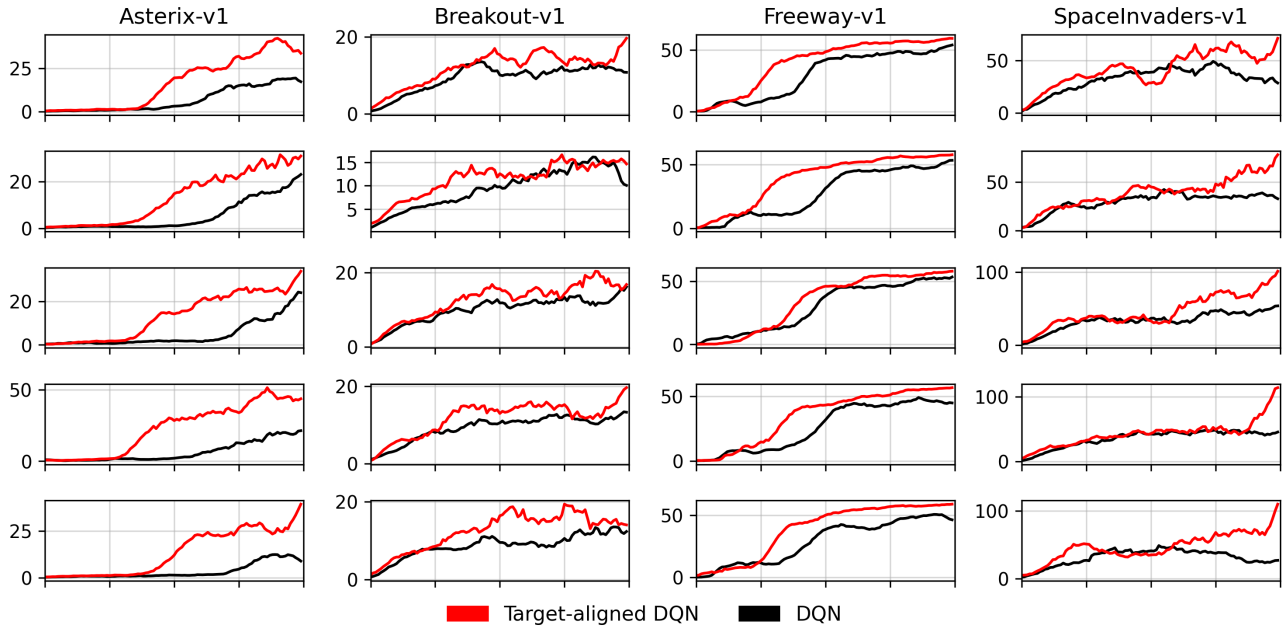


Figure 5. Per-seed performance comparison between DQN and target-aligned DQN on four games of the MINATAR benchmarks. Curves represent returns, smoothed over 10 points.

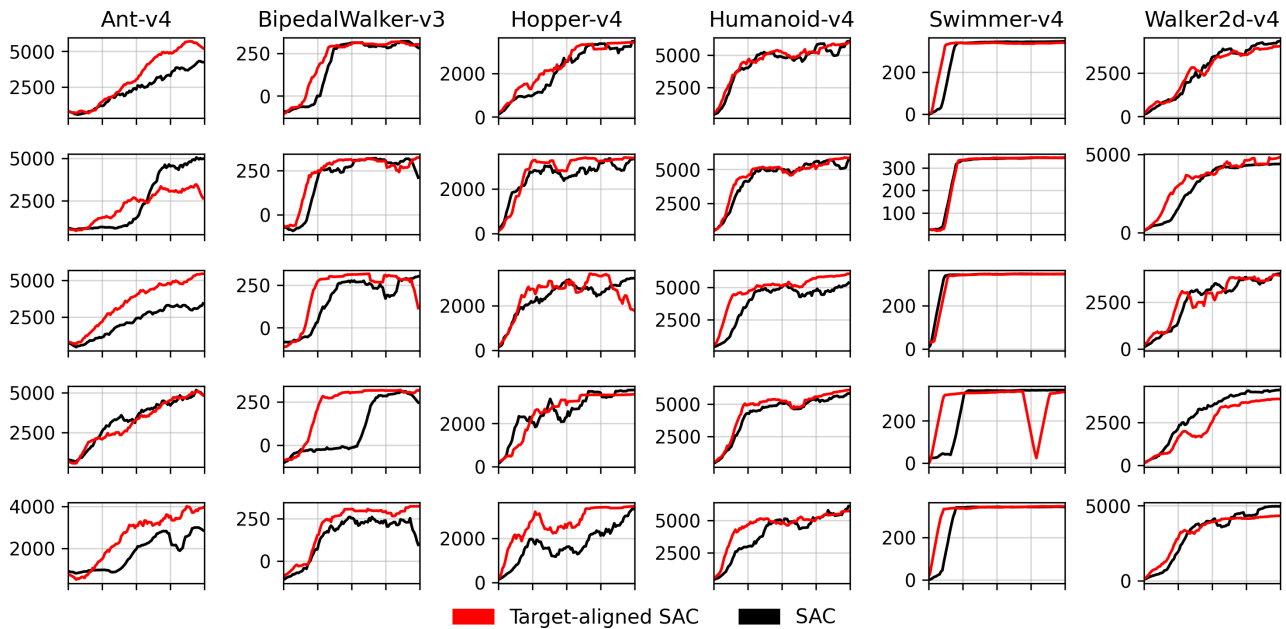


Figure 6. Per-seed performance comparison between SAC and target-aligned SAC on six games of the MINATAR benchmarks. Curves represent returns, smoothed over 10 points.